NJC

ROYAL SOCIETY OF CHEMISTRY

PAPER

View Article Online
View Journal | View Issue

Cite this: *New J. Chem.*, 2023, **47**, 12697

Effect of ions on the adsorption of lysozyme protein below its isoelectric point on hydrophilic (OH–Si) and hydrophobic (H–Si) surfaces

Sanu Sarkar, Aditi Saikia and Sarathi Kundu *

Lysozyme is a rigid globular protein with four disulfide bonds that is present in human tears, saliva, sweat and milk. In the present study, thin films of this protein are deposited on hydrophilic (OH–Si) and hydrophobic (H–Si) silicon surfaces using the dip coating method. In order to study the effect of ions, these films were also fabricated by varying the concentration of mono-(Na^+), di-(Ca^{2+}) and tri-(Y^{3+}) valent ions. The structural and topographical characteristics of these films are investigated using X-ray reflectivity (XRR) and atomic force microscopy (AFM) techniques and are correlated with the surface hydrophobicity/hydrophilicity. On a OH–Si surface, a thick layer of lysozyme (≈47 Å) is adsorbed in the absence of ions. However, in the presence of 1–10 mM of ions the thickness varied from ≈40 to 61 Å. Conversely, the thickness of the lysozyme film in the absence of any ions on the hydrophobic H–Si surface is ≈57 Å, which varied in the range of ≈44 to 69 Å in the presence of ions. Mostly, a bi-molecular layer is formed on the substrate surface where the substrate-attached lower layer molecules are in the side-on orientation (≈24 Å) and on top of that one more layer is formed where the molecules are either in side-on orientation or tilted with respect to the lower layer. On the OH–Si surface, pure or ion-interacted lysozyme films are adsorbed in their native globular form with almost negligible structural modification. However, on the H–Si surface, the globular shape of the adsorbed lysozyme molecules is slightly elongated mostly due to the presence of the relatively higher hydrophobic interaction between the protein and H–Si surface. The hydrophobic nature of the protein films as obtained from the contact angle studies showed that on the OH–Si surface the contact angle of the lysozyme film interacting with Na^+ ions is the highest, whereas it is intermediate and the lowest for Y^{3+} and Ca^{2+} ions, respectively. Moreover, the contact angle of the lysozyme film is the highest for Ca^{2+} and the lowest for Na^+ ions on the H–Si surface. Therefore, the thicker protein films exhibit more hydrophobic nature and the contact angle varies in accordance with the electron density of the adsorbed films.

Received 9th February 2023,
Accepted 20th May 2023

DOI: 10.1039/d3nj00624g

rsc.li/njc

1. Introduction

Ions are ubiquitously present in living ecosystems starting from living organisms to marine systems, and they (ions or salts) play a vital role in controlling various physicochemical processes, *e.g.*, signal transduction of neurons,[1] antibacterial functioning,[2] lipid digestion,[3] cell adhesion,[4] cellular signaling,[5] enzymatic catalysis,[6] muscular contraction,[7,8] oxygen transport,[9] protein separation, purification, crystallization,[10–12] *etc.* However, some toxic ions impart adverse effects on the human body, *e.g.*, Pb^{2+} contributes to neurotoxicity in cellular signaling,[5] Hg^{2+} and Cd^{2+} cause biological toxicity,[13,14] *etc.* Blood, which is the most important fluid that flows inside the circulatory tracks of living creatures, also interacts with ions. Although ions constitute only ≈ 1% weight of total human plasma,[15] they perform some vital functions, *e.g.*, Fe^{2+} (or Fe^{3+}) ions that undergo reversible Fe^{2+}(or Fe^{3+})-oxygen bond formation help to dissolve oxygen in the blood and then transport that to different parts of living organisms.[9] Amongst the different types of ions that are present in body fluid, namely Na^+, K^+, Mg^{2+}, Ca^{2+}, Mn^{2+}, Cu^{2+}, Zn^{2+}, Fe^{2+}(or Fe^{3+}), Cl^-, HCO_3^-, SO_4^{2-} and PO_4^{3-} ions, the Na^+, Ca^{2+} and Cl^- ions are the majority and they maintain plasma osmolarity and muscle contraction.[15–17] In short, it should be accepted that biological processes are mostly controlled by ions. Therefore, the insertion of artificial systems, like implants, stents, *etc.* into the living body results in different ion-mediated protein interactions or protein adsorptions. Ions present in living fluid perform some vital functions, *e.g.*, Na^+ ions participate in exchange of ions with the surroundings to regulate electrochemical potential, fluid–electrolyte balance, and acid–base balance in extracellular fluid, whereas Ca^{2+} ions bind with actin and expose the binding site for myosin,

Soft Nano Laboratory, Physical Sciences Division, Institute of Advanced Study in Science and Technology (IASST), Vigyan Path, Paschim Boragaon, Garchuk, Guwahati, Assam 781035, India. E-mail: sarathi.kundu@gmail.com; Fax: +91 361 2279909; Tel: +91 361 2912075

which helps in muscle contraction.[7,17] Although yttrium (Y^{3+}) ions are not present in the living body but they can enter through inhalation, which causes liver edema, pleural effusions, and pulmonary hyperemia.[18] In fact, to control different biological functions and to mimic the adsorption of proteins in actual living organisms, the inclusion of the effects of ions on protein adsorption is necessary.

Adsorption of one such globular protein lysozyme is also controlled under different ion interactions. Along with the type and concentration of interacting ions, the other factors that affect the adsorption of lysozyme on a solid surface are wettability, roughness and chemical composition of the substrate surface; pH, concentration and temperature of the protein solution, *etc.*[12,19–21] The effect of different factors like ion interaction and surface wettability was explored in our previous work where we investigated the effect of ions on the adsorption of a negatively charged globular protein bovine serum albumin (BSA) on a hydrophilic surface.[22] However, an understanding of the effects of ions on positively charged protein molecules on hydrophilic or hydrophobic surfaces is lacking. Therefore, studies on the adsorption of smaller and positively charged globular protein lysozyme on slightly negatively charged hydrophilic (OH–Si) and slightly positively charged hydrophobic (H–Si) surfaces in the presence of different ions will be effective as it will present a suitable model of the mechanism of protein–surface and protein–protein interaction with the help of amino acid residues. Lysozyme is used here as a model protein as it has structural similarity with some other proteins found in living organisms and in addition, it is commercially available at low cost.

Published literature on lysozyme adsorption shows that in the absence or in the presence of low concentration of ions, proteins undergo irreversible monolayer adsorption, while intermediate or high concentrations of ions help to stabilize multilayer adsorption.[22–24] In the multilayer form, each layer of lysozyme possesses a different structural conformation and orientation, *i.e.*, the first layer adsorbs with side-on orientation with more conformational change compared to the second layer having end-on orientation.[25] It is reported that a monolayer of lysozyme (side-on) has been adsorbed on a hydrophilic surface while a bi- or tri-layer has been deposited on a hydrophobic surface.[26] Lower adsorption of lysozyme on hydrophilic (negatively charged) silica surfaces was recorded with increasing ionic strength of monovalent Na^+ ions, because of ionic screening between the protein and silica surface.[18] Negatively charged globular protein RNase A undergoes higher adsorption in the presence of Mg^{2+} ions compared to Na^+ ions on TiO_2 and SiO_2 surfaces as reported by Wendorf *et al.*[27] In another work by Zanna *et al.*, higher adsorption of negatively charged BSA was found on stainless steel surfaces in the presence of 10 mM of divalent ions (Mg^{2+}, Ca^{2+}) compared to monovalent (Na^+) ions.[28] The effect of ions on protein adsorption can also be understood using a sequence of ions, which is called the Hofmeister series. Ions which cause salting in (chaotropes) increase the solubility of proteins by weakening the protein–protein hydrophobic interactions, whereas salting out is caused by kosmotropic ions, which decrease the solubility of the proteins by enhancing the protein–protein hydrophobic interaction. When adsorption of protein takes place in the presence of such ions, the increase or decrease of protein solubility increases or decreases the amount of protein adsorption on hydrophilic or hydrophobic solid surfaces.[29] Anionic proteins like BSA above their isoelectric point (IEP) follow the Hofmeister series.[30] However, cationic proteins like lysozyme (below IEP), follow the reverse Hofmeister series at moderate or low ion concentrations.[29–32]

The hydrophilicity/hydrophobicity of solid surfaces plays an important role in the adsorption of lysozyme on solid–liquid interfaces. Lysozyme molecules contain both hydrophilic as well as hydrophobic regions and have an IEP at $\approx$11.2, which indicates that lysozyme possesses net positive and negative surface charge below or above pH $\approx$ 11.2, whereas it is neutral at the IEP.[33] This makes lysozyme adsorption favorable on both hydrophilic as well as hydrophobic surfaces *via* hydrophobic as well as electrostatic interactions.[34,35] The capability of lysozyme in aqueous solution to adhere on hydrophilic or hydrophobic surfaces depends on the structural arrangement or configuration of lysozyme and also on the intensity of removing the hydrating water layer over the solid surface.[24] Generally, on hydrophobic surfaces, a thicker layer of lysozyme is formed compared to the hydrophilic surface,[36] whereas with increasing hydrophilicity lysozyme undergoes lower adsorption.[37] The structure of the adsorbed lysozyme on different surfaces depends on the protein–protein and protein–surface interactions, which are different for different surfaces of varying hydrophobicity. Strong hydrophobic interaction between the surface and the hydrophobic amino acid residues of lysozyme stabilizes its structure. On intermediate hydrophobic surfaces, the combined effects of protein–protein and protein–surface interaction contribute to determining the adsorbed protein structure.[20] Although different studies are there on protein adsorption, in most of the studies the adsorption processes are performed in aqueous media and the wet protein films are characterized using *in situ* techniques.[34,38–40] However, the dried protein (lysozyme) film undergoes a negligible change in structure with temperature variation.[41,42] Dried lysozyme films can be used for antibacterial studies and can also be effectively utilized as a 2D template for 3D protein crystallization.[43] Dried films of BSA adsorbed on metallic surfaces can act as an effective lubricating agent by minimizing the friction co-efficient.[44]

The current study is designed with the aim of investigating (i) the adsorption of lysozyme *via ex situ* methods, (ii) the role of different valent ions and their valency, (iii) the effect of ion concentration and (iv) the effect of surface wettability (hydrophilicity/hydrophobicity) on lysozyme adsorption on solid silicon surfaces. The work is performed by (i) adsorbing the protein films on solid surfaces by dip coating and characterizing them by different *ex situ* methods, (ii) choosing mono-, di- and trivalent ions, *i.e.*, Na^+, Ca^{2+} and Y^{3+} and (iii) by varying the concentration of the salts/ions from 0 to 10 mM at a fixed protein concentration of 15 mg mL^{-1} and solution pH of $\approx$7.0. All the salts used here have a common anion Cl^- with different cations Na^+, Ca^{2+} and Y^{3+}; therefore, the effect of cations will be more relevant to compare the structure of

adsorbed lysozyme films. Moreover, Na^+ and Ca^{2+} cations are chosen for their significant role in the metabolism of the body, whereas Y^{3+} is chosen for its toxic effects towards proteins in the body. Therefore, it will be informative to check whether the lysozyme adsorption is followed by the Hofmeister series or by some other properties, *e.g.*, charge density, electronegativity, valency of ions, *etc.* Furthermore, XRR and AFM are applied to study the structure and morphology of the adsorbed lysozyme films while the hydrophilicity/hydrophobicity is studied by water contact angle measurement and their respective results are reported and discussed with suitable scientific explanation using the state of the art literature.

2. Experimental details

2.1. Materials

Lysozyme from chicken egg white (catalog No. 62971) and Yttrium(III) chloride hexahydrate ($YCl_3{\cdot}6H_2O$, $M_w \approx 303.36$ g mol^{-1}, 99.99%) were purchased from Sigma Aldrich and were used without further purification. Ammonia solution 25% (NH_4OH, $M_w \approx 17.03$ g mol^{-1}), hydrogen peroxide (H_2O_2) 30% (H_2O_2, $M_w \approx 34.01$ g mol^{-1}), hydrofluoric acid 40% (HF, $M_w \approx 20.01$ g mol^{-1}, CAS No-7664-39-3), sodium chloride (NaCl, $M_w \approx 58.44$ g mol^{-1}, 99%) and calcium chloride dihydrate ($CaCl_2{\cdot}2H_2O$, $M_w \approx 147.02$ g mol^{-1}, 97%) were purchased from Merck.

2.2. Preparation of hydrophilic silicon (OH–Si) surface

Silicon (001) substrates of appropriate size were cut and then cleaned with acetone. The substrates were then subjected to boiling at 100 °C in a solution containing a mixture of Milli-Q water, 25% NH_4OH and 30% H_2O_2 in the ratio of 2 : 1 : 1 for 5–8 min to render the silicon substrates hydrophilic.

2.3. Preparation of a hydrophobic silicon (H–Si) surface

Silicon (001) substrates of appropriate sizes were cleaned with acetone properly. HF 40% solution was mixed with Milli-Q water in the ratio 1 : 3 to change the concentration to 10%. The cleaned substrates were then dipped in the 10% HF solution for 3 min at room temperature (25 °C). After removing the substrates from the solution, they were rinsed in 50 mL Milli-Q water for 5 min.

2.4. Preparation of thin films of lysozyme

Stock solution of 30 mg mL^{-1} lysozyme solution was prepared by adding hen egg white lysozyme powder in Milli-Q water in the appropriate ratio. Stock solutions of 20 mM of NaCl, $CaCl_2$ and YCl_3 salts were also prepared. The stock solutions of lysozyme and the salts were mixed to form 15 mg mL^{-1} of lysozyme solution accompanied with 1, 5 and 10 mM of NaCl, $CaCl_2$ and YCl_3. The freshly prepared OH–Si and H–Si surfaces were dipped immediately in 4 mL of the salt mixed lysozyme solutions for 20 min and then dried for 24 h and then rinsed in Milli-Q water for 5 min. The protein adsorbed substrates were then dried and used for further characterizations (Scheme 1). All the processes of lysozyme deposition were done at room temperature (25 °C).

The present study uses ionic concentration up to 10 mM considering the normal concentration of ions in the intra cellular or extra cellular body fluid. The concentration of Na^+ ions in the intra cellular and extra cellular fluid is around 12–14 mM and 140–145 mM respectively and that of Ca^{2+} ions is around 0.01–0.1 μM and 2.2–2.6 mM respectively.[44–46] Furthermore, in the diseased or abnormal metabolism condition of the body fluid, the normal values of ion concentration may change to show the concentrations from 0 to 10 mM. The chosen range of ionic concentration is also effective in controlling the thickness of the adsorbed protein films and protein stability, and in

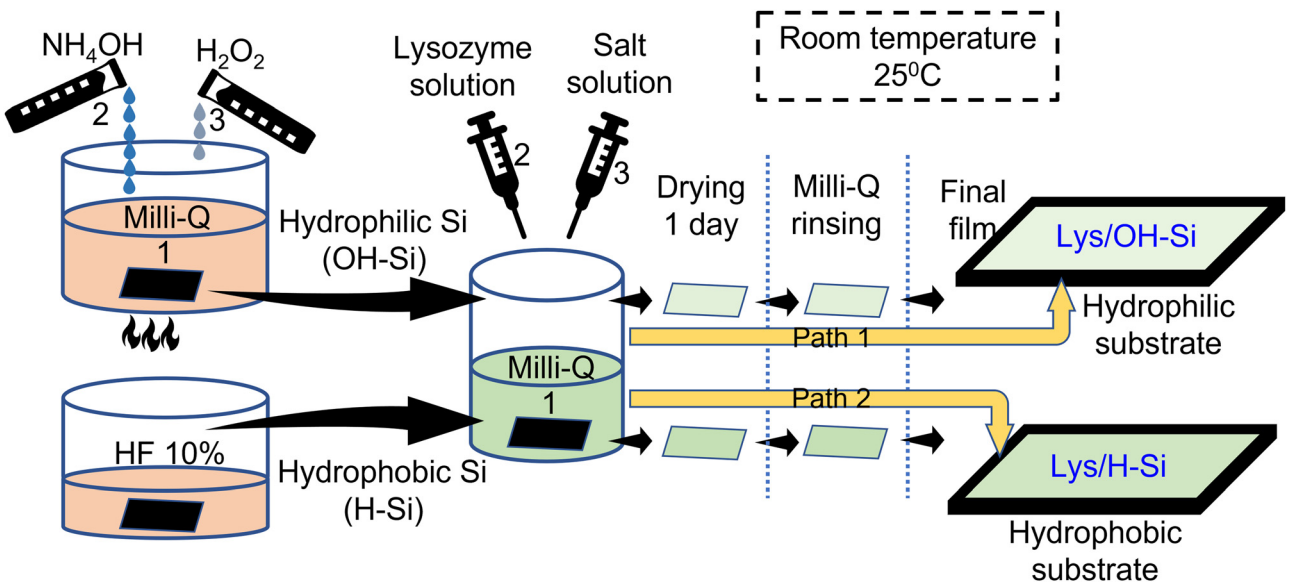

Scheme 1 Preparation of lysozyme ultrathin films on OH–Si and H–Si surfaces.

addition will eliminate the screening effect to favour lysozyme adsorption. A relatively higher concentration of lysozyme (15 mg mL^{-1}) was chosen to favour enough interaction of the protein molecules with the substrate surface to undergo adsorption. The selected protein concentration approximately matches with the synovial liquids of patients and the periprosthetic fluid under chronic inflammatory conditions, which is around 8–13 mg mL^{-1}.[47]

2.5. XRR characterization

To obtain the XRR profiles of all the adsorbed protein films, a D8 Advanced, Bruker, AXS (XRD) set-up was used which uses Cu K_α radiation (λ = 1.54 Å). K_α radiation was incident onto the x–y plane of the prepared films at low angles and the reflected radiation was collected using a NaI scintillation detector fulfilling the specular condition. The reflectivity data were recorded against the z-component (q_z) of the wave vector as shown below,

$$q_z = (4\pi/\lambda)\sin\theta \quad (1)$$

The data were fitted using Parratt's formalism, in which a film is considered as a stack of layers, and the surface and interface roughness were introduced.[48] The electron density profiles (EDPs) obtained from the data fitting give the out-of-plane structure of the deposited films.[49]

2.6. AFM analysis

NTEGRA Prima, NT-MDT Technology working in the semi-contact mode was employed to get the AFM image from an area of 2 μm × 2 μm of the film. It uses a silicon cantilever (spring constant ≈ 11.8 N m^{-1}) and laser beam in the constant force mode.[50] The variation of the tip-surface distance was used to obtain the topography of the scan area. With the use of WSxM software, recorded AFM images were analyzed.[51]

2.7. Contact angle analysis

The pure and ion interacted lysozyme films adsorbed over OH–Si and H–Si surfaces were used for the contact angle analysis using a KRUSS Contact Angle Analyzer. The sessile drop method was used to record the water contact angles of the protein films. A sessile drop of Milli-Q water of volume 10 μL was dropped onto each protein surface at a rate of 0.50 μL s^{-1}. Contact angles were recorded at 5 different places of each protein surface so that the mean angle gives the final contact angle.

3. Results and discussion

The structural and morphological properties of the pure lysozyme films deposited on OH–Si and H–Si surfaces are investigated with the help of XRR and AFM studies. The presence of intermolecular interactions between the protein molecules and substrate as shown in Scheme 2, helped in the formation of thin layered lysozyme films as reported in Wei *et al.*,[20] Latour *et al.*[23] and Anastas *et al.*[52] In the OH–Si surface, the amino acids with hydrophilic moieties like aspartic acid (Asp, $-CH_2-COOH$), serine (Ser, $-CH_2-COOH$), glutamic acid (Glu, $-CH_2-CH_2-COOH$), lysine (Lys, $H_2N-(CH_2)_4$), *etc.* attached to the

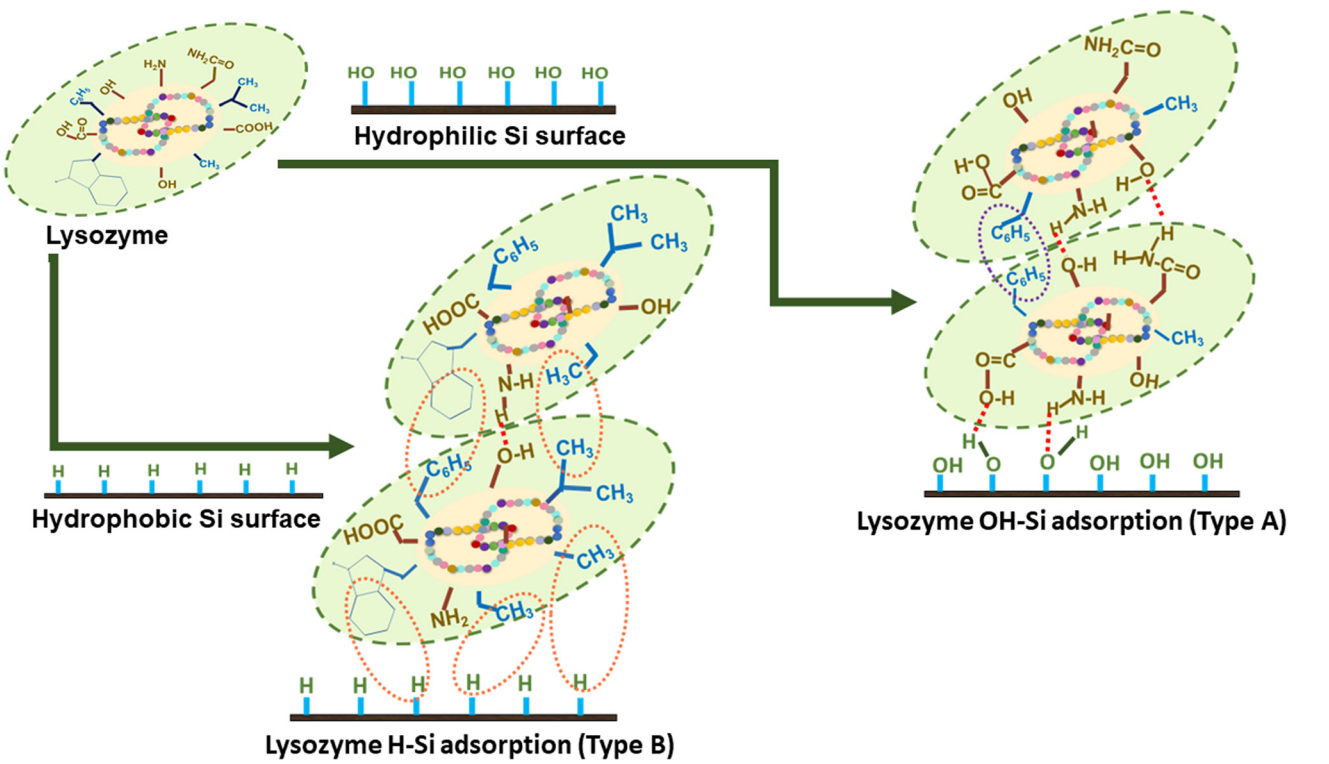

Scheme 2 Schematic representation of plausible lysozyme-lysozyme and lysozyme-surface interactions during adsorption on OH–Si (Type A) and H–Si (Type B) surfaces.

silicon surface *via* oxygen resulting in the formation of either donor or acceptor type hydrogen bonds, as shown in Scheme 2. On the contrary, on the H–Si surface, the lysozyme molecule consisting of nonpolar moieties like $-CH_2-C_6H_5$, $-CH_3$, and $-CH-(CH_3)_2$ in the amino acids result in the formation of hydrophobic interactions with the H–Si surface. Also, the presence of such hydrophobic interactions between the proteins further stabilizes the tertiary structure of the protein on the Si surfaces. In addition to this, both hydrophobic as well as hydrophilic interactions are present that help to form a bilayer-like structure of proteins over the Si surfaces. Scheme 2 shows the interaction of lysozyme molecules with the OH–Si and H–Si surface as well as interactions between other lysozyme molecules.

Related scheme of adsorption of different concentrations of human milk lysozyme on a hydrophilic silicon oxide (SiO_2) surface using a dual polarization interferometer and quartz crystal microbalance was also earlier proposed by K Xu *et al.*[53] However, they proposed different side-on, edge-on and end-on orientations of lysozyme molecules along with trapped solvent in the lysozyme monolayer at various surface coverages. However, in this study, we have proposed different orientations of lysozyme molecules embedded in the lysozyme bilayer on the hydrophilic surface without any trapped solvent. The XRR data (open circles) combined with the fitted curves (solid lines) and the EDPs (extracted from the fitting of the XRR data), and the corresponding AFM images are shown in Fig. 1(a–d). The EDPs implied that the maximum electron densities of pure protein films are obtained as $\approx$ 0.46 and 0.51 electrons $Å^{-3}$, whereas the thicknesses are found to be $\approx$ 47 Å and 57 Å on OH–Si and H–Si surfaces, respectively. Adsorption of a thicker protein layer on the hydrophobic surface than the hydrophilic surface in the absence of ions is due to the higher hydrophobic interaction between the protein and surface. The average and total heights as obtained from the height histogram and height scale bar of the pure lysozyme films are $\approx$ 2.05 and 3.53 nm on OH–Si surface, whereas $\approx$ 2.62 and 4.46 nm on H–Si surfaces, respectively.

XRR analysis is also applied to find the out-of-plane structural information of the ion-interacted lysozyme films deposited on hydrophilic and hydrophobic surfaces. Similar XRR studies were performed in previous works of Richter *et al.* where they studied the lysozyme adsorption on hydrophilic SiO_2 and hydrophobic OTS–Si surfaces and found that lysozyme molecules adsorb in side-on orientation on hydrophilic surfaces while they denature on highly hydrophobic OTS surfaces but they did not propose any pictorial presentation to understand the adsorption and did not study the effect of ions.[40] Lu *et al.* also studied lysozyme adsorption on hydrophobic OTS–Si surfaces but did not study the effect of ions, and while they propose different side-on or end-on orientations of lysozyme molecules, the interfacial layer structure was not shown.[34] Hahl *et al.*[54] presented a scheme for the adsorption of lysozyme on hydrophilic SiO_2 and hydrophobic OTS–Si substrates. Although it considered the monolayer/bilayer model in aqueous medium over SiO_2 and OTS modified silicon using the *in situ* XRR method, the effect of ions was not verified. Evers *et al.*[55] on the other hand, also presented a scheme of lysozyme film

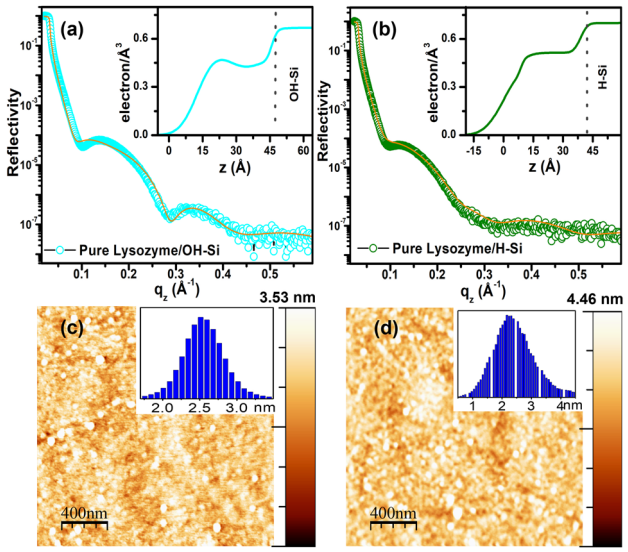

Fig. 1 XRR curves (open circle) combined with the fitted curves (solid line) and EDP (a and b) and AFM images (c and d) of pure lysozyme films adsorbed on a OH–Si surface (a and c) and H–Si surface (b and d).

formation on a hydrophilic OH–Si surface but it describes a monolayer model in aqueous medium characterized by the *in situ* XRR method. It was not supported by other characterizations and the effect of ions was not examined. However, we have explored the effect of different ions on the adsorption of lysozyme on hydrophilic and hydrophobic surfaces by *ex situ* XRR along with other methods (AFM, Contact angle) and presented a bilayer model of lysozyme molecules in dried form over OH–Si and H–Si surfaces. Possible mechanisms of protein–protein, protein–surface interactions and protein tilting with suitable schemes and diagrams are also discussed. The XRR data (open circles) and the corresponding fitted curves (solid lines) and EDPs of the lysozyme films deposited on the OH–Si surface are shown in Fig. 2(a–f). In Fig. 2(a), the XRR data with fitted curves are shown, while the EDPs as shown in Fig. 2(d) indicate that $\approx$ 61 Å, 44 Å and 48 Å thick lysozyme layers are formed in the presence of 1 mM of mono- (Na^+), di- (Ca^{2+}) and tri-valent (Y^{3+}) ions respectively. Their maximum electron densities vary from 0.41 to 0.53 electrons $Å^{-3}$. Under the interaction of the same three valent ions for 5 mM concentration, nearly 51 Å, 40 Å and 44 Å thick lysozyme layers are formed, which are shown in Fig. 2(e). The maximum electron densities in the adsorbed film vary from 0.24 to 0.50 electrons $Å^{-3}$. However, in the presence of 10 mM ion concentration, $\approx$ 48 Å, 44 Å and 44 Å thick lysozyme layers are deposited for the same three ions and the maximum electron densities in the adsorbed films vary from 0.25 to 0.27 electrons $Å^{-3}$. The corresponding XRR data and EDPs are shown in Fig. 2(c) and (f) respectively. It is clear from the EDPs that for 1 and 5 mM, the shapes of the EDPs of the ion-interacted lysozyme films are different from each other and their thickness also varies from each other, while for 10 mM ion concentration the shapes of the EDPs almost resemble each other and show nearly equal thickness. Thus, the out-of-plane

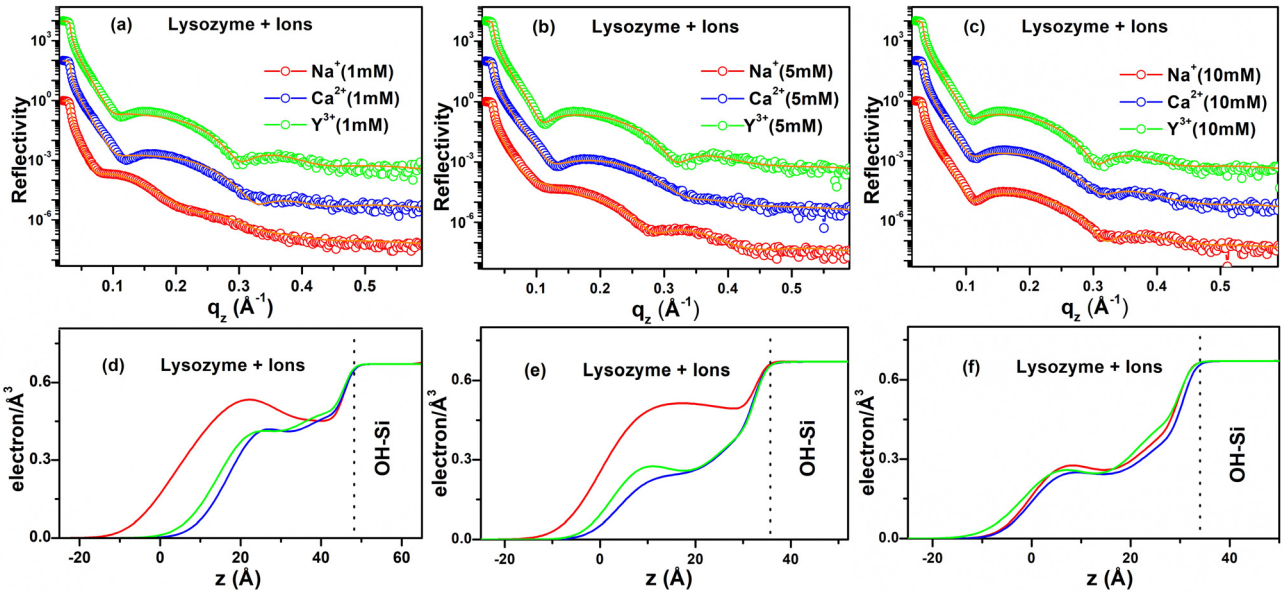

Fig. 2 XRR curves (open circles) combined with the fitted curves (solid lines) of 1 mM (a), 5 mM (b) and 10 mM (c) and the corresponding EDPs (d–f) of different ion interacted lysozyme films adsorbed on the OH–Si surface.

structures of the adsorbed protein layer on OH–Si are mostly dependent on the specific valent ions and also on their concentration. The thickness of the adsorbed lysozyme layer on the OH–Si surface for a particular ion decreases as the concentration of ions increases, which is in accordance with an earlier report.[56] The decrease in protein adsorption with increasing ion concentration is attributed to greater screening of the charge of lysozyme and the OH–Si surface, which causes weaker electrostatic interaction.[27] However, variation of adsorption with different valence ions may be related to the amount of exposure of hydrophilic residues of lysozyme at that particular ionic environment, which may interact with the OH–Si surface.

The structural features of the ion-interacted lysozyme films adsorbed on the H–Si surface are achieved by XRR measurements. The XRR data (open circles), fitted curves (solid lines) and corresponding EDPs are shown in Fig. 3(a–f). The XRR data (Fig. 3(a)) and EDPs extracted from the data fitting of the lysozyme films in the presence of 1 mM of Na^{+}, Ca^{2+} and Y^{3+} ions give a total thickness of ≈ 44 Å, 54 Å and 54 Å respectively on the H–Si surface (shown in Fig. 3(d)). The maximum electron density varies from 0.45 to 0.51 electrons $Å^{-3}$. At the

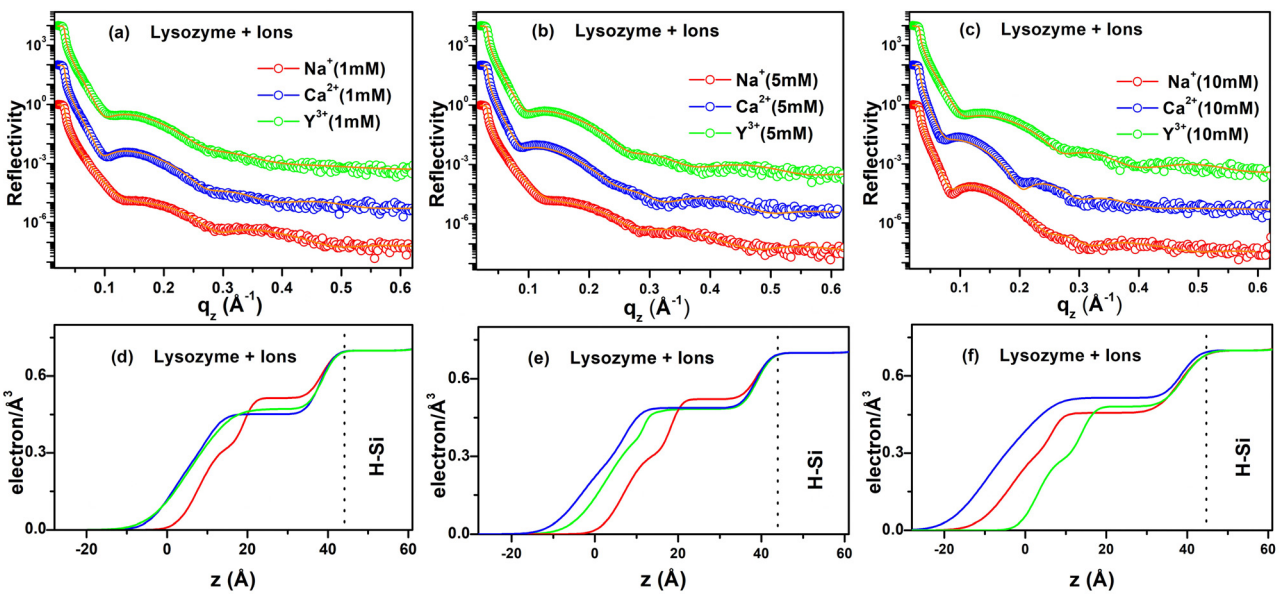

Fig. 3 XRR curves (open circles) combined with the fitted curves (solid lines) of 1 mM (a), 5 mM (b) and 10 mM (c) and the corresponding EDPs (d–f) of different ion interacted lysozyme films adsorbed on the H–Si surface.

intermediate concentration (5 mM) of the three valent ions, the XRR data obtained from the deposited films on the H–Si surface are shown in Fig. 3(b) and the corresponding EDPs are shown in Fig. 3(e), which indicates ≈ 46 Å, 61 Å and 56 Å thick adsorbed protein films, respectively. Moreover, the maximum electron density varies from 0.48 to 0.52 electrons $Å^{-3}$. At a concentration of 10 mM of Na^+, Ca^{2+}, and Y^{3+} ions, the XRR data obtained from the adsorbed protein films are shown in Fig. 3(c) and the corresponding EDPs are shown in Fig. 3(f) from which it is clear that ≈ 62 Å, 69 Å and 48 Å thick protein layers are adsorbed on the H–Si surface in the presence of the three ions, respectively, and the maximum electron density varies from 0.45 to 0.51 electrons $Å^{-3}$. Form the EDPs of the protein films on hydrophobic H–Si it is obvious that the film thickness is lower in the presence of Na^+ ions, intermediate for Y^{3+} ions and maximum for Ca^{2+} ions. Thus, like hydrophilic surfaces, the adsorption here is primarily ion specific. Although, in the presence of a specific ion, when the ion concentration is increased the adsorption of lysozyme increases on hydrophobic surfaces. The increase in adsorption is due to higher hydrophobic interaction between the non-polar residues of lysozyme and the surface with the addition of ions.[27,57] Although, hydrophobic interaction is dominant, the effect of other interactions cannot be ignored.

AFM studies have also been used along with XRR to find the morphology of lysozyme films on OH–Si and H–Si surfaces in the presence of ions. Several literature studies were reported on the utilization of AFM for understanding the adsorption mechanism of protein films; however, these studies were reported mostly only on the pure proteins.[36] Here, we have studied the ion effect of three different ions (Na^+, Ca^{2+} and Y^{3+}) by AFM analysis of adsorbed lysozyme films on OH–Si and H–Si surfaces and the results are shown in Fig. 4(a–i) and Fig. 5(a–i), respectively. The average and total heights of each film on OH–Si are shown by the height histograms (in inset) and Z-scale bars (on right-hand side) respectively in Fig. 4(a–i). At 1 mM ion concentration, the average and total heights of the films are obtained as ≈ 2.54 and 4.32 nm for Na^+ ions, ≈ 1.97 and 2.92 nm for Ca^{2+} ions and ≈2.05 and 3.56 nm for Y^{3+} ions. At 5 and 10 mM salt concentrations, the average and total heights also become maximum for Na^+ ions, and then for Y^{3+} and Ca^{2+} ions, respectively. The average and total heights of the adsorbed lysozyme films on

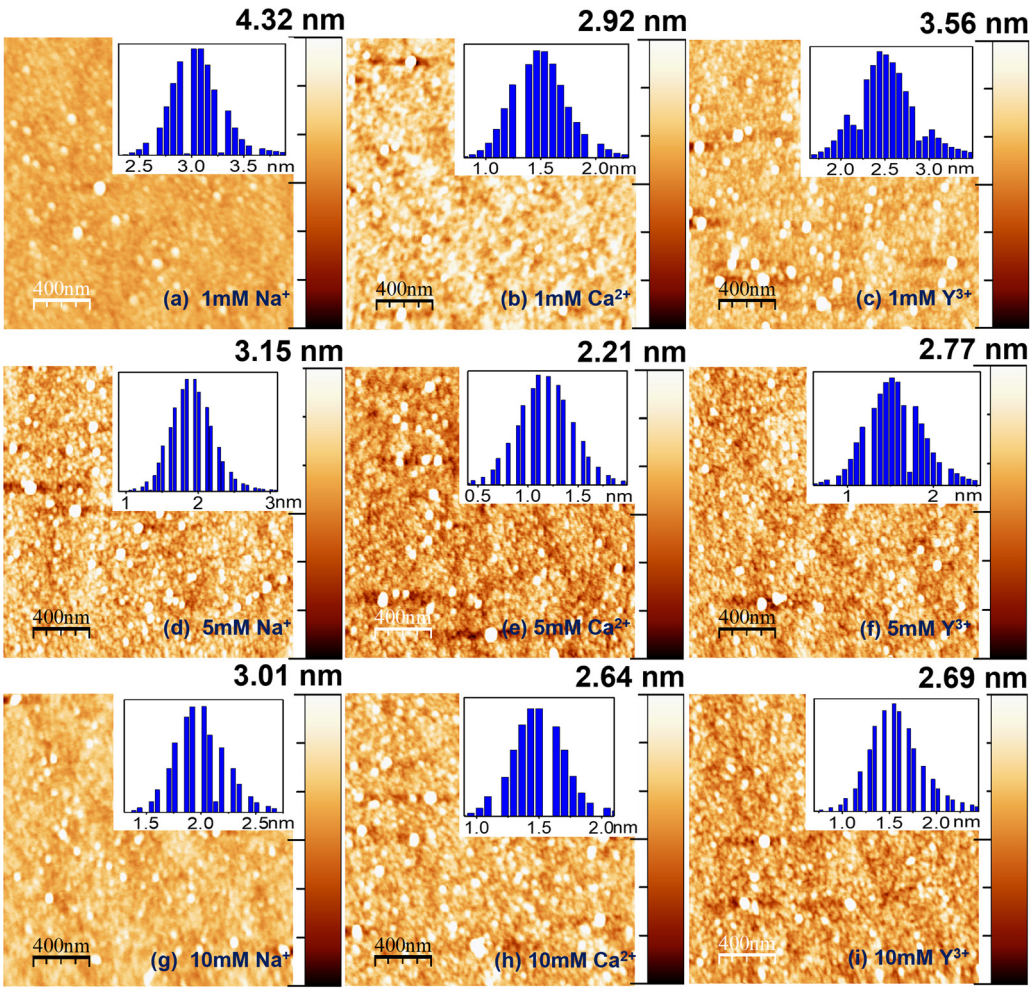

Fig. 4 AFM images of lysozyme films on the OH–Si surface modified by 1 mM (a–c), 5 mM (d–f) and 10 mM (g–i) of different ions. Right columns: Z-scale bars. Insets: Height histograms.

the OH–Si surface for all the ions at different concentrations are indicated in Table 1.

The morphology of the adsorbed lysozyme films on H–Si in the presence of Na^+, Ca^{2+} and Y^{3+} ions is shown in Fig. 5(a–i). Unlike OH–Si, for the H–Si surface, the maximum height of the adsorbed protein layer is obtained for Ca^{2+} ions. At 10 mM salt concentration, the maximum average and total heights of the protein films are obtained as $\approx$ 3.36 and 4.80 nm for Ca^{2+} ions. The average and total heights of the adsorbed lysozyme films on the H–Si surface for all the different conditions are tabulated in Table 1. On the OH–Si surface, the least height is recorded for Ca^{2+} ions, while for the same ions, the adsorbed height is recorded as maximum on the H–Si surface. The r.m.s. roughnesses obtained from AFM studies and out-of-plane roughness of the top surface obtained from XRR studies of all the films on OH–Si and H–Si surfaces are also mentioned in Table 1. From the AFM images it is also clear that for the lysozyme films adsorbed on the OH–Si surface the native globular form is maintained with almost no structural modification, while on the H–Si surface, although the globular shape of lysozyme molecules is maintained, some amount of structural modification may take place due to the presence of higher hydrophobic interaction between lysozyme and the H–Si surface, and probably for that on the H–Si surface the shape of the globules becomes slightly elongated. Due to dominant hydrophobic interaction between the protein and the hydrophobic surface, more proteins are adsorbed on the hydrophobic surface than the hydrophilic one in the absence of any ions. On both surfaces, protein molecules are almost uniformly distributed in the presence or absence of ions due to the combined effects of hydrophobic, hydrophilic and electrostatic interactions between the lysozyme molecules and substrate surface.[58]

The water contact angle of the bare OH–Si surface is obtained as 20.0° (Fig. 6(a)) before dipping inside the protein solution and after depositing pure lysozyme film on it, the water contact angle becomes 69.0° (Fig. 6(b)). In the presence of Na^+ ions, the contact angles of the lysozyme films become 73.6°, 68.0° and 64.5° for 1, 5 and 10 mM salt concentration (details in Table 2), and among them the contact angle of 68.0° for 5 mM is shown in Fig. 6(c). In the presence of Ca^{2+} ions, the contact angle changes from 64.1° to 62.2° as the concentration changes from 1 to 5 mM, and finally becomes 62.0° at 10 mM. Whereas, for Y^{3+} ions, the

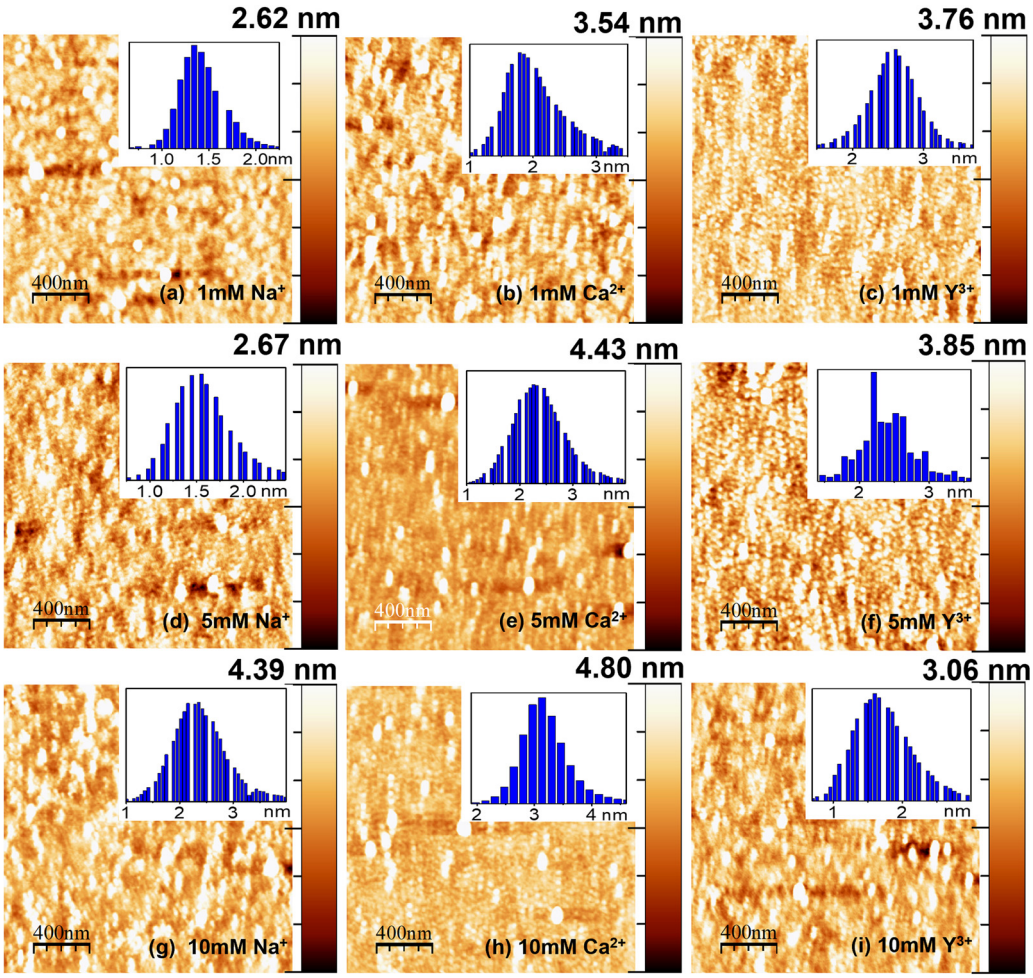

Fig. 5 AFM images of lysozyme films on H–Si surfaces modified by 1 mM (a–c), 5 mM (d–f) and 10 mM (g–i) of different ions. Right columns: Z-scale bars. Insets: Height histograms.

Table 1 Average heights, total heights, rms roughnesses and out-of-plane roughnesses of lysozyme films adsorbed on OH–Si (H–Si) surfaces in the presence of Na^+, Ca^{2+}, Y^{3+} ions (from 1 to 10 mM). All the height and roughness values of lysozyme films adsorbed on the H–Si surface are mentioned within the brackets

			Types of ions		
OH–Si surface (H–Si surface)	PureLys/OH–Si (PureLys/H–Si) (nm)	Ion concentration	Na^+ (nm)	Ca^{2+} (nm)	Y^{3+} (nm)
Average height	2.05 (2.62)	1 mM	2.54 (1.87)	1.97 (2.54)	2.05 (2.63)
		5 mM	1.99 (1.89)	1.56 (3.16)	1.74 (2.68)
		10 mM	1.99 (3.15)	1.64 (3.36)	1.68 (1.95)
Total height	2.05 (2.62)	1 mM	4.32 (2.62)	2.92 (3.54)	3.56 (3.76)
		5 mM	3.15 (2.67)	2.21 (4.43)	2.77 (3.85)
		10 mM	3.01 (4.39)	2.64 (4.80)	2.69 (3.06)
Rms roughness	0.45 (0.40)	1 mM	0.52 (0.32)	0.35 (0.53)	0.42 (0.48)
		5 mM	0.46 (0.41)	0.32 (0.56)	0.40 (0.49)
		10 mM	0.42 (0.45)	0.28 (0.64)	0.38 (0.51)
Out-of-plane roughness (top surface)	0.64 (0.76)	1 mM	0.70 (0.42)	0.70 (0.51)	0.77 (0.75)
		5 mM	0.64 (0.42)	0.50 (0.60)	0.50 (0.65)
		10 mM	0.50 (0.64)	0.49 (0.71)	0.68 (0.35)

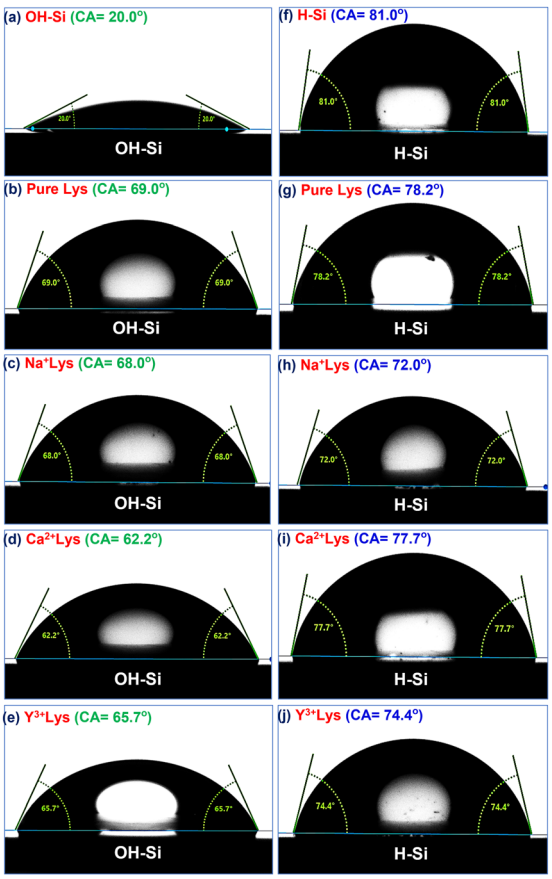

Fig. 6 Static water contact angles of (a) the OH–Si surface; (b–e) pure, Na^+, Ca^{2+}, and Y^{3+} ion (5 mM) interacted lysozyme films adsorbed onto the OH–Si surface; (f) the H–Si surface; (g–j) pure, Na^+, Ca^{2+}, Y^{3+} ion (5 mM) interacted lysozyme films adsorbed onto the H–Si surface.

contact angle becomes 68.4°, 65.7° and 63.6° for 1, 5 and 10 mM salt concentration respectively. The contact angles for both Ca^{2+} and Y^{3+} ions (at 5 mM) are shown in Fig. 6(d) and (e) respectively. The water contact angle of the H–Si surface is obtained as 81.0° (Fig. 6(f)) and after deposition of pure lysozyme film on it, the water contact angle becomes 78.2° (Fig. 6(g)). In the presence of

Table 2 Static water contact angle values of bare and protein adsorbed OH–Si and H–Si surfaces in the presence of Na^+, Ca^{2+}, Y^{3+} ions (from 1 to 10 mM)

		Type of surface	
Ion	Concentration	OH–Si	H–Si
Pure	0 mM	69.0°	78.2°
Na^+	1 mM	73.6°	70.5°
	5 mM	68.0°	72.0°
	10 mM	64.5°	76.6°
Ca^{2+}	1 mM	64.1°	75.0°
	5 mM	62.2°	77.7°
	10 mM	62.0°	80.0°
Y^{3+}	1 mM	68.4°	74.1°
	5 mM	65.7°	74.4°
	10 mM	63.6°	74.8°

Na^+, Ca^{2+} and Y^{3+} ions, the contact angle of the protein film changes from 70.5° to 76.6°, from 75.0° to 80.0° and from 74.1° to 74.8° respectively as the ion concentration varies from 1 to 10 mM. The contact angles of the adsorbed lysozyme films on the H–Si surface for Na^+, Ca^{2+} and Y^{3+} ions (at 5 mM) are shown in Fig. 6(h), (i) and (f), respectively. The values of contact angle on both the OH–Si and H–Si surfaces for different conditions are tabulated in Table 2. Thus, the presence of ions changes the hydrophobicity of the lysozyme films on both hydrophilic OH–Si and hydrophobic H–Si surfaces.

The contact angles of protein films adsorbed on OH–Si and H–Si surfaces in the presence of different ions of varying concentration are plotted in Fig. 7(a and b). These plots are quite similar to the variations of the integrated values of the EDPs, as shown in Fig. 7(c and d). Therefore, it is obvious that on the hydrophilic surface, the attachment of a thicker protein layer in the presence of Na^+ ions contributes to the highest water contact angle value, while the lowest and intermediate thicknesses of the attached protein films in the presence of Ca^{2+} and Y^{3+} ions cause the lowest and intermediate contact angles respectively. Almost the opposite trend is obtained by protein films on the hydrophobic surface where the contact angle is the highest for Ca^+ ions compared to Na^+ and Y^{3+} ions, respectively. Attachment of a thin protein layer due to lower

lysozyme adsorption in the presence of divalent Ca^{2+} cations or attachment of a thicker protein layer due to higher lysozyme adsorption in the presence of monovalent Na^+ cations on the OH–Si surface (Fig. 7(a and c)) may be correlated with a sequence of ions known as the reverse Hofmeister series which is the opposite of the Hofmeister series.[29] In the reverse Hofmeister series, the salting-in to salting-out behavior follows the specific order of cations, *i.e.*, $Cs^+ > Rb^+ > K^+ > Na^+ > Li^+ > Mg^{2+} > Ca^{2+}$. The solubility of a cationic protein like lysozyme (below IEP) follows the reverse Hofmeister series at moderate or low ion concentration.[31,32] Accordingly, monovalent Na^+ cations have much higher salting-in (chaotropic) properties compared to divalent Ca^{2+} cations or divalent Ca^{2+} cations have much higher salting-out (kosmotropic) properties compared to monovalent Na^+ cations. Therefore, Na^+ ions cause higher solubility of lysozyme than Ca^{2+} ions which means relatively higher exposure of the hydrophilic residues and as a result in the presence of monovalent Na^+ cations, lysozyme undergoes higher adsorption on hydrophilic surfaces. The phenomenon of higher solubility of cationic protein lysozyme at a low concentration of monovalent (Na^+) cations compared to divalent (Mg^{2+}) cations having a common anion (Cl^-) has been previously reported as well by Ries-Kautt *et al.*[59] The reverse phenomenon occurs for the H–Si surface (Fig. 7(b and d)) and as a result due to the exposure of more hydrophobic residues in the presence of Ca^{2+} ions, lysozyme undergoes higher adsorption on the hydrophobic surface. Intermediate adsorption of lysozyme on both the surfaces in the presence of trivalent Y^{3+} ions is beyond the scope of the Hofmeister series. However, we can propose that in the presence of Y^{3+} ions, lysozyme may have intermediate solubility between Na^+ and Ca^{2+} cations and hence undergoes intermediate adsorption on both hydrophilic and hydrophobic silicon surfaces. Again, higher (lower) adsorption of lysozyme at lower (higher) concentration of ions on the hydrophilic surface is consistent with the previous studies. Lower concentration of ions enables a more compact structure of the lysozyme, allowing less space (voids) for the solvent to be trapped within the protein and hence more protein molecules get a chance to interact with the surface to get adsorbed more.[19,60]

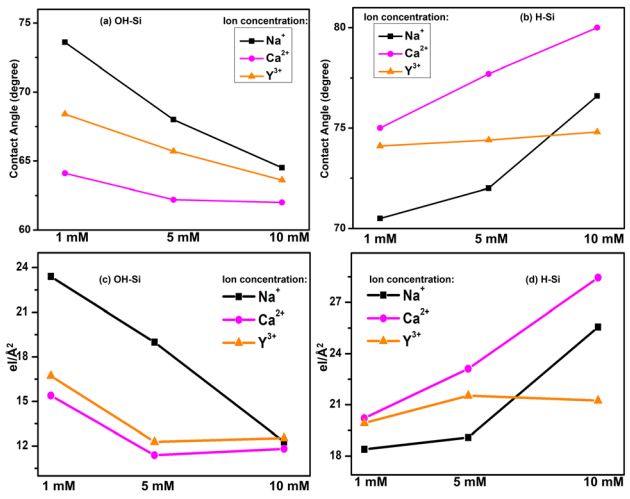

Fig. 7 Comparison of static water contact angle (a and b) and the integrated values as obtained from the EDPs (c and d) of 1–10 mM of Na^+, Ca^{2+} and Y^{3+} ion interacted lysozyme films adsorbed on OH–Si and H–Si surfaces.

Table 3 Thickness of protein films on OH–Si and H–Si surfaces in the presence of Na^+, Ca^{2+}, and Y^{3+} ions (from 1 to 10 mM). Maximum error for the film thickness is obtained as 3–7%

		Type of surface	
Ions	Concentration	OH–Si (Å)	H–Si (Å)
Pure	0 mM	47 ± 2 (24 + 23)	57 ± 2 (24 + 33)
Na^+	1 mM	61 ± 4 (24 + 37)	44 ± 3 (24 + 20)
	5 mM	51 ± 3 (24 + 27)	46 ± 2 (24 + 22)
	10 mM	48 ± 2 (24 + 24)	62 ± 2 (24 + 38)
Ca^{2+}	1 mM	44 ± 3 (24 + 20)	54 ± 3 (24 + 30)
	5 mM	40 ± 2 (24 + 16)	61 ± 3 (24 + 37)
	10 mM	44 ± 2 (24 + 20)	69 ± 2 (24 + 45)
Y^{3+}	1 mM	48 ± 2 (24 + 24)	54 ± 2 (24 + 30)
	5 mM	44 ± 2 (24 + 20)	56 ± 2 (24 + 32)
	10 mM	44 ± 1 (24 + 20)	48 ± 2 (24 + 24)

If we consider the structure of the lysozyme molecule as a prolate spheroid of dimensions $a \times b \times b \approx 27.8$ Å $\times$ 11.8 Å $\times$ 11.8 Å,[61] then the total thickness as obtained from the XRR analysis may provide the number of lysozyme layers in the adsorbed films. If the lysozyme is adsorbed on the substrate surface with side-on orientation, then one molecular layer thickness will be around 24–26 Å, while for the end-on orientation the thickness of one molecular layer will be around 55–57 Å. Thus, the thickness as shown in Table 3 implies that mostly a bi-molecular layer is adsorbed on the substrate surface in the presence of all three ions, whereas for the substrate-attached first layer (lower layer) the molecules are in the side-on orientation (thickness $\approx$ 24 Å) and on top of that one upper layer is formed where the molecules are either in side-on orientation or tilted with respect to the lower layer as the thickness will be more than 24 Å, which is also shown in Table 3 within brackets. The amount of such molecular tilting is relatively less on the OH–Si surface in comparison with the H–Si surface. The structure of the adsorbed bi-molecular layer on the OH–Si and H–Si surfaces is shown schematically in Fig. 8(i–iv) respectively. However, on the OH–Si surface, the higher molecular tilting or thicker upper layer is formed for Na^+ ions and on the H–Si surface such higher molecular tilting or thicker upper layer is formed for Ca^+ ions. The results of the above study may be evaluated for protein

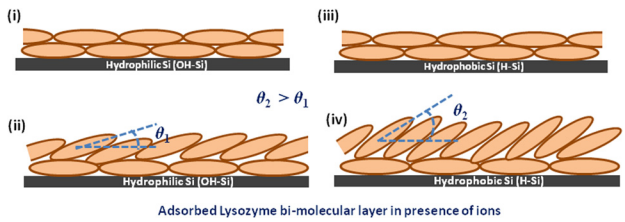

Fig. 8 Bi-molecular layer structure of lysozyme films on OH–Si and H–Si surfaces. The tilting angle of the upper molecular layer on the H–Si surface (θ_2) is higher than that on the OH–Si surface (θ_1).

sensing, protein crystallization, non-specific adsorption, nucleation, biomaterial surface design, anti-bacterial studies, *etc.*

4. Conclusions

The effect of mono-(Na^+), di-(Ca^{2+}) and tri-(Y^{3+}) valent ions on the structure and morphology of a lysozyme layer adsorbed on hydrophilic (OH–Si) and hydrophobic (H–Si) surfaces is studied. In the absence of ions, an $\approx$ 47 Å thick layer of protein film is deposited on the OH–Si surface, while in the presence of 1–10 mM of Na^+, Ca^{2+} and Y^{3+} ions, $\approx$ 40 to 61 Å thick protein layers are formed. But on H–Si surface, an $\approx$ 57 Å thick protein film is deposited in the absence of any ions and in the presence of the three ions, an $\approx$ 44 to 69 Å thick protein layers are formed. Mostly, a bi-molecular layer is formed on both the OH–Si and H–Si surfaces, where in the substrate-attached lower layer the molecules are in side-on orientation and in the upper layer the molecules are either in side-on orientation or tilted with respect to the lower layer. On both OH–Si and H–Si surfaces, the native globular form of the protein is nearly maintained in the absence or presence of ions; however, on the H–Si surface the molecules are slightly elongated mostly due to hydrophobic interaction between the protein and the surface. The hydrophobic nature of the protein films as obtained from the contact angle studies shows that on the OH–Si surface the contact angle of the lysozyme film interacted by Na^+ ions is the highest, whereas it is intermediate and the lowest for Y^{3+} and Ca^{2+} ions, respectively, but on the H–Si surface, it is the highest for Ca^{2+} and the lowest for Na^+ ions. Thus, the probable structure, morphology and hydrophobicity of adsorbed lysozyme molecules on both hydrophilic and hydrophobic silicon surfaces in the presence of mono-(Na^+), di-(Ca^{2+}) and tri-(Y^{3+}) valent ions are explored and the same are also investigated with the variation of ion concentration.

Author contributions

S. Sarkar and S. Kundu conceived the concept, methodology and sample preparation/synthesis together. S. Sarkar performed the characterization, data collection and plotting. S. Sarkar and A. Saikia contributed to writing the first draft of the manuscript and all authors reviewed the whole manuscript to approve the final version of the manuscript.

Conflicts of interest

The authors declare that there are no conflicts of interest.

Acknowledgements

The authors acknowledge Sophisticated Analytical Instrument Centre (SAIC), IASST for the characterization facilities. S. Sarkar wants to acknowledge the Council of Scientific and Industrial Research (CSIR), New Delhi, India, for financial assistance through the CSIR SRF Fellowship [File number-09/835(0030)/2019-EMR-I]. Dr A. Saikia and Dr S. Kundu wants to acknowledge the financial assistance provided by the Department of Science and Technology, Govt. of India.

References

1 A. Ono, S. Cao, H. Togashi, M. Tashiro, T. Fujimoto, T. Machinami, S. Oda, Y. Miyake, I. Okamoto and Y. Tanaka, *Chem. Commun.*, 2008, 4825–4827.
2 Y. Wang, F. Wang, H. Zhang, B. Yu, H. Cong and Y. Shen, *Appl. Mater. Today*, 2021, **25**, 101192.
3 A. I. Mulet-Cabero and P. J. Wilde, *Crit. Rev. Food Sci. Nutr.*, 2021, 1–14.
4 P. B. Armstrong, *J. Exp. Zool.*, 1966, **163**, 99–109.
5 A. Garza, R. Vega and E. Soto, *Med. Sci. Monit.*, 2006, **12**, RA57–RA65.
6 M. Vašák and J. Schnabl, in *The Alkali Metal Ions: Their Role for Life*, ed. A. Sigel, H. Sigel, and R. Sigel, Springer, Cham, 2016, vol. 16, 259–290.
7 S. Ebashi and M. Endo, *Prog. Biophys. Mol. Biol.*, 1968, **18**, 123–183.
8 R. S. Filo, D. F. Bohr and J. C. Ruegg, *Science*, 1965, **147**, 1581–1583.
9 C. Thomas and A. B. Lumb, *Crit. Care Pain Med.*, 2012, **12**, 251–256.
10 K. D. Collins, *Methods*, 2004, **34**, 300–311.
11 A. Sauter, F. Roosen-Runge, F. Zhang, G. Lotze, R. M. Jacobs and F. Schreiber, *J. Am. Chem. Soc.*, 2015, **137**, 1485–1491.
12 N. Amaly, Y. Ma, A. Y. El-Moghazy and G. Sun, *Sep. Purif. Technol.*, 2020, **250**, 117086.
13 M. D. Miyamoto, *Brain Res.*, 1983, **267**, 375–379.
14 S. Yoshida, *Brain Res.*, 2001, **892**, 102–110.
15 H. M. Kim, K. Kishimoto, F. Miyaji, T. Kokubo, T. Yao, Y. Suetsugu, J. Tanaka and T. Nakamura, *J. Biomed. Mater. Res.*, 1999, **46**, 228–235.
16 P. M. May, P. W. Linder and D. R. Williams, *J. Chem. Soc., Dalton Trans.*, 1977, **6**, 588–595.
17 X. Zheng, W. Cheng, C. Ji, J. Zhang and M. Yin, *Rev. Anal. Chem.*, 2020, **39**, 231–246.
18 K. T. Rim, K. H. Koo and J. S. Park, *Saf. Health Work*, 2013, **4**, 12–26.
19 M. Lundin, U. M. Elofsson, E. Blomberg and M. W. Rutland, *Colloids Surf., B*, 2010, **77**, 1–11.
20 Y. Wei, A. A. Thyparambil and R. A. Latour, *Colloids Surf., B*, 2013, **110**, 363–371.
21 H. E. Ei, Y. Nakama, H. Tanaka, H. Imanaka, N. Ishida and K. Imamura, *Colloids Surf., B*, 2016, **147**, 9–16.
22 S. Sarkar and S. Kundu, *JCIS Open*, 2021, **3**, 100016.
23 R. A. Latour, *Colloids Surf., B*, 2020, **191**, 110992.
24 P. Komorek, M. Wałek and B. Jachimska, *Bioelectrochemistry*, 2020, **135**, 107582.
25 A. M. Vervald, E. N. Vervald, S. A. Burikov, S. V. Patsaeva, N. A. Kalyagina, N. E. Borisova, I. I. Vlasov, O. A. Shenderova and T. A. Dolenko, *J. Phys. Chem. C*, 2020, **124**, 4288–4298.
26 M. Malmsten, *Colloids Surf., B*, 1995, **3**, 297–308.
27 J. R. Wendorf, C. J. Radke and H. W. Blanch, *Colloids Surf., B*, 2010, **75**, 100–106.

28 S. Zanna, C. Compère and P. Marcus, in 9th International Symposium, *Passivation of Metals and Semiconductors, and Properties of Thin Oxide Layers*, ed. P. Marcus and V. Maurice, Elsevier Science, Paris, France, 2006, pp. 365–370.
29 Y. F. Yano, Y. Kobayashi, T. Ina, K. Nitta and T. Uruga, *Langmuir*, 2016, **32**, 9892–9898.
30 N. Schwierz, D. Horinek and R. R. Netz, *Langmuir*, 2013, **29**, 2602–2614.
31 Y. Zhang and P. S. Cremer, *Proc. Natl. Acad. Sci. U. S. A.*, 2009, **106**, 15249–15253.
32 A. Salis, M. S. Bhattacharyya and M. Monduzzi, *J. Phys. Chem. B*, 2010, **114**, 7996–8001.
33 R. J. Sarmah and S. Kundu, *Food Hydrocolloids*, 2022, 107788.
34 J. R. Lu, T. J. Su, P. N. Thirtle, R. K. Thomas, A. R. Rennie and R. Cubitt, *J. Colloid Interface Sci.*, 1988, **206**, 212–223.
35 S. Zhang and Y. Sun, *Biotechnol. Prog.*, 2004, **20**, 207–214.
36 G. M. L. Messina, C. Satriano and G. Marletta, *Colloids Surf., B*, 2009, **70**, 76–83.
37 L. Yi, K. Xu, G. Xia, J. Li, W. Li and Y. Cai, *Appl. Surf. Sci.*, 2019, **480**, 923–933.
38 F. Evers, R. Steitz, M. Tolan and C. Czeslik, *J. Phys. Chem. B*, 2009, **113**, 8462–8465.
39 M. R. Fries, D. Stopper, M. K. Braun, A. Hinderhofer, F. Zhang, R. M. Jacobs, M. W. Skoda, H. Hansen-Goos, R. Roth and F. Schreiber, *Phys. Rev. Lett.*, 2017, **119**, 228001.
40 A. G. Richter and I. Kuzmenko, *Langmuir*, 2013, **29**, 5167–5180.
41 E. Pechkova, P. Innocenzi, L. Malfatti, T. Kidchob, L. Gaspa and C. Nicolini, *Langmuir*, 2007, **23**, 1147–1151.
42 A. A. Thyparambil, Y. Wei and R. A. Latour, *Biointerphases*, 2015, **10**, 019002.
43 E. Pechkova and C. Nicolini, *Nat. Protoc.*, 2017, **12**, 2570–2589.
44 A. I. Masyuk, T. V. Masyuk and N. F. LaRusso, in Physiology of Cholangiocytes, *Physiology of the Gastrointestinal Tract (Fifth Edition)*, ed. L. R. Johnson, J. D. Kaunitz, H. M. Said, F. K. Ghishan, J. L. Merchant, J. D. Wood, Academic Press, 2012, vol. 2, pp. 1531–1557.
45 D. K. Atchison and W. H. Beierwaltes, *Pflug. Arch. Eur. J. Phy.*, 2013, **465**, 59–69.
46 A. L. Lehninger, D. L. Nelson and M. M. Cox, Lehninger principles of biochemistry, *Biological membranes and transport*, Macmillan, 4th edn, 2005.
47 A. P. Serro, R. Colaço and B. Saramago, *ACS Symp. Ser. Am. Chem. Soc.*, 2012, **1120**, 497–523.
48 L. G. Parratt, *Phys. Rev.*, 1954, **95**, 359–369.
49 S. Kundu, A. Datta, M. K. Sanyal, J. Daillant, D. Luzet, C. Blot and B. Struth, *Phys. Rev. E: Stat., Nonlinear, Soft Matter Phys.*, 2006, **73**, 061602.
50 K. Das and S. Kundu, *Colloids Surf., A*, 2016, **492**, 54–61.
51 I. Horcas, R. Fernández, J. M. Gómez-Rodríguez, J. Colchero, J. Gómez-Herrero and A. M. Baró, *Rev. Sci. Instrum.*, 2007, **78**, 013705.
52 P. T. Anastas, A. Rodriguez, T. M. de Winter, P. Coish and J. B. Zimmerman, *Green Chem. Lett. Rev.*, 2021, **14**, 302–338.
53 K. Xu, M. M. Ouberai and M. E. Welland, *Biomaterials*, 2013, **34**, 1461–1470.
54 H. Hähl, F. Evers, S. Grandthyll, M. Paulus, C. Sternemann, P. Loskill, M. Lessel, A. K. Hüsecken, T. Brenner, M. Tolan and K. Jacobs, *Langmuir*, 2012, **28**, 7747–7756.
55 F. Evers, K. Shokuie, M. Paulus, C. Sternemann, C. Czeslik and M. Tolan, *Langmuir*, 2008, **24**, 10216–10221.
56 T. J. Su, J. R. Lu, R. K. Thomas, Z. F. Cui and J. Penfold, *J. Colloid Interface Sci.*, 1998, **203**, 419–429.
57 W. Norde and J. Lyklema, *J. Colloid Interface Sci.*, 1978, **66**, 257–265.
58 Y. F. Yano, T. Uruga, H. Tanida, Y. Terada and H. Yamada, *J. Phys. Chem. Lett.*, 2011, **2**, 995–999.
59 M. M. Ries-Kautt and A. F. Ducruix, *J. Biol. Chem.*, 1989, **264**, 745–748.
60 J. Buijs and V. Hlady, *J. Colloid Interface Sci.*, 1997, **190**, 171–181.
61 S. Pandit, S. Kundu, S. Abbas, V. K. Aswal and J. Kohlbrecher, *Chem. Phys. Lett.*, 2018, **711**, 8–14.

